Journal of Molecular Catalysis A: Chemical 372 (2013) 29–34

Contents lists available at SciVerse ScienceDirect

Journal of Molecular Catalysis A: Chemical

journal homepage: www.elsevier.com/locate/molcata

A comparative study about the effects of isomorphous substitution of transition metals (Ti, Cr, Mn, Co and Ni) on the UV/Fenton catalytic activity of magnetite

Yuanhong Zhong[a,c], Xiaoliang Liang[a], Wei Tan[a,c], Yin Zhong[b], Hongping He[a,*], Jianxi Zhu[a], Peng Yuan[a], Zheng Jiang[d]

[a] Key Laboratory of Mineralogy and Metallogeny, Guangzhou Institute of Geochemistry, Chinese Academy of Sciences, Guangzhou 510640, China
[b] Pearl River Delta Research Center of Environment Pollution and Control, Guangzhou Institute of Geochemistry, Chinese Academy of Sciences, Guangzhou 510640, China
[c] University of Chinese Academy of Sciences, Beijing 100049, China
[d] Shanghai Institute of Applied Physics, Chinese Academy of Sciences, Shanghai 201800, China

ARTICLE INFO

Article history:
Received 6 November 2012
Accepted 26 January 2013
Available online 14 February 2013

Keywords:
Magnetite
Isomorphous substitution
Catalytic activity
UV/Fenton
TBBPA

ABSTRACT

Magnetite catalysts doped by five common transition metals (Ti, Cr, Mn, Co and Ni) on a similar level were prepared by a precipitation–oxidation method and characterized by chemical analysis, XRD, TG-DSC, BET surface area and XANES. The effects of substituting metal species on the photocatalytic performance of magnetite were investigated and compared through the UV/Fenton degradation of tetrabromobisphenol A (TBBPA). The substitution of above metals improved the heterogeneous UV/Fenton degradation of TBBPA, and the improvement extent increased in the following order: Co < Mn < Ti ≈ Ni < Cr. Fewer intermediate product species were detected in the systems with higher degradation efficiency. The distinct effects of these substituting metals on the UV/Fenton catalytic activity of magnetite were discussed in terms of reaction mechanism and surface property varieties. The substituting cations participated in the H_2O_2 decomposition through Haber–Weiss mechanism and enhanced separation and transfer efficiency of the photo-generated electrons and holes, both of which improved the generation of $^{\bullet}OH$ free radicals. Furthermore, with larger specific surface area and higher surface hydroxyl amount, substituted magnetite exhibited stronger catalytic activity for TBBPA degradation.

1. Introduction

With the merits of strong catalytic activity, great reserves and excellent environmental compatibility, magnetite has been widely applied in environmental remediation in these years [1–5], and its role in environmental self-purification also has become a research hotspot [6,7]. In the natural world, partial iron ions in the inverse spinel structure of magnetite are isomorphously replaced by some transition metal ions, e.g. Ti^{4+} [8], Cr^{3+} [9], Mn^{2+} [10], Co^{2+} [11], and Ni^{2+} [10]. Previous studies have investigated the effect of above substitutions on the heterogeneous Fenton catalytic activity of magnetite, which was greatly dependent on the occupancy, nature and amount of substituting metals [12–14]. For example, the catalytic activity relied on the octahedral cations rather than the tetrahedral ones, as the octahedral sites were almost exclusively exposed at the surface of inverse spinel structure [14]. Cr^{3+}, Co^{2+} and Mn^{2+} obviously increased the $^{\bullet}OH$ production for organic pollutant degradation by Fenton reaction, while Ni^{2+} and Ti^{4+} inhibited this process [8,10]. This was ascribed to the fact that the former cations accelerated the electronic transfer to produce the active specie Fe^{2+} for the Fenton reaction, but the latter ones were thermodynamically unfavorable to reduce Fe^{3+} to Fe^{2+} [8–10]. However, these tested magnetite catalysts were not prepared by the same method, neglecting the influence of synthesis methods on the catalytic activity of prepared samples.

Recently, photocatalysis of UV/Fenton by magnetite has attracted great attentions, owing to the fact that the introduction of ultraviolet light into Fenton system obviously improved the pollutant degradation and mineralization. Our recent study has investigated the UV/Fenton catalytic activity of titanomagnetite ($Fe_{3-x}Ti_xO_4$) for tetrabromobisphenol A (TBBPA) degradation [15]. TBBPA was a widely used brominated flame retardant, one of persistent organic pollutants (POPs) with negative influence on various aspects of mammalian and human physiology [16–19]. Ti^{4+} substitution in magnetite greatly improved the UV/Fenton degradation of TBBPA on neutral pH condition, and the degradation efficiency increased with the increment of titanium content [15]. Under the best condition, almost complete degradation of

* Corresponding author. Present address: Guangzhou Institute of Geochemistry, Chinese Academy of Sciences, 511 Kehua Street, Guangzhou 510640, China. Tel.: +86 20 85290257; fax: +86 20 85290130.
E-mail address: hehp@gig.ac.cn (H. He).

1381-1169/$ – see front matter © 2013 Elsevier B.V. All rights reserved.
http://dx.doi.org/10.1016/j.molcata.2013.01.038

TBBPA was accomplished with the main degradation pathways of sequential debromination and mineralization. With the advantages of strong catalytic activity, easy recycle by magnetism and excellent environmental harmony, titanomagnetite was considered as a promising catalyst for TBBPA removal. However, to the best of our knowledge, little attention has been paid to the effect of other substituted transition metals on the catalytic activity of magnetites for POPs degradation (e.g. TBBPA). This is of high importance for well understanding the role of natural doped magnetite in environmental self-purification and preparation of efficient catalysts for POPs degradation.

In the present study, magnetites substituted by different transition metals (Ti, Cr, Mn, Co and Ni) to a similar extent were prepared by a precipitation-oxidation method [20]. The effects of these substitutions on the UV/Fenton catalytic activity of magnetite were compared through a series of TBBPA degradation experiments, and the reaction mechanisms were discussed. The obtained results are of great significance for the application of magnetite group minerals in the UV/Fenton degradation of TBBPA and helpful for us to well understand the environmental fate of TBBPA in the natural world.

2. Experimental

2.1. Synthesis and characterization of catalysts

All the chemicals and reagents used in this study were of analytical grade and were used as received. The magnetite samples $Fe_{3-x}M_xO_4$ (M = Fe, Ti, Cr, Mn, Co and Ni) were synthesized by a precipitation–oxidation method as described in literatures [8,15,21]. The concentration ratio between iron and substituting metal (Fe:M) was about 2:1 in the initial acid solution.

The contents of Fe and substituting metals (M) in the synthetic samples were determined by using Varian Vista inductively coupled plasma atomic emission spectroscopy (ICP-AES). Powder X-ray diffraction (PXRD) patterns were recorded between 10° and 80° (2θ) at a step of 1° per minute on a Bruker D8 advance diffractometer with Cu K_α radiation (40 kV and 40 mA). BET specific surface area was measured on the basis of N_2 physisorption capacity at 77 K on an ASAP 2020 instrument, after degassed at 433 K for 12 h. X-ray absorption near-edge structure (XANES) spectra were obtained on the new Wiggler beamline BL14W1 of Shanghai Synchrotron Radiation Facility (SSRF). The storage ring was operated at 3.5 GeV electron energy and 150–300 mA beam current. The BL14W1 was a focused X-ray beamline, using a Si (1 1 1) double crystal monochromator. The K-edge absorption spectra of all the samples were recorded in the transmission mode. Thermogravimetric and differential scaning calorimetry (TG-DSC) analyses were synchronously performed on a Netzsch STA 409 PC instrument. Approximately 10 mg of finely ground sample was heated in a corundum crucible with a heating rate 10 °C min^{-1} under N_2 atmosphere. The leaching Fe ion concentration during TBBPA degradation was analyzed on a PE-3100 flame atomic absorption spectrophotometer (FAAS).

2.2. UV/Fenton degradation of TBBPA

TBBPA degradation through heterogeneous UV/Fenton reaction was carried out in a home-made photo-reactor with a 6W UV-light tube (λ = 365 nm) [22]. Methanol was chosen as the hydrotropic agent to increase the solubility of TBBPA, which was propitious to observe the TBBPA transformation process. The volume ratio of methanol to water was optimized at 2:3 in the preliminary experiment. Before degradation, the suspension containing magnetite sample (0.5 g L^{-1}) and TBBPA (20 mg L^{-1}) was stirred for 60 min in dark to make the particles and TBBPA well dispersed.

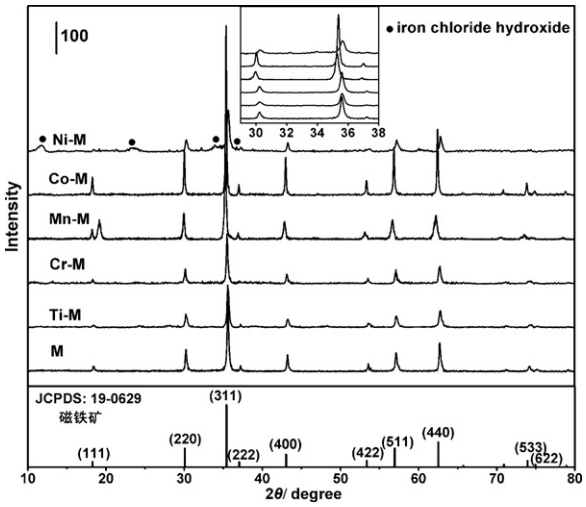

Fig. 1. X-ray diffraction patterns of synthetic $Fe_{3-x}M_xO_4$ samples.

The degradation was initiated by simultaneously adding H_2O_2 and turning on the UV light. At given intervals, the reaction solution was sampled for TBBPA concentration analysis and intermediate product identification.

The TBBPA concentration was analyzed by a Shimadzu LC-20A high performance liquid chromatography (HPLC), equipped with an Inertisil ODS-SP column (150 mm × 4.6 mm, 5 μm particles). The mobile phase was a mixture of methanol and 0.2% glacial-acetic-acid solution at a volumetric ratio of 4:1. The flow rate was set at 0.8 mL min^{-1} and the wavelength of UV detection was set at 222 nm. The degradation products of TBBPA were analyzed by gas chromatographic mass spectrometry (GC–MS), equipped with a Rxi-5ms fused silica capillary column (DB-5MS, 30 m × 0.25 mm × 0.25 μm). The oven temperature program was initiated at 80 °C for 1 min, raised at a rate of 5 °C min^{-1} to 300 °C and then held for 10 min. Helium was used as the carrier gas at a flow rate of 1 mL min^{-1}. Mass spectra were recorded in the electron ionization mode with electron energy of 70 eV and the ion source and MS interface temperature were maintained at 250 and 280 °C, respectively. The inlet was held isothermally at 260 °C and injections were set in the split mode of 10:1.

3. Results and discussion

3.1. Characterization of magnetite samples

From the chemical analysis results, the chemical formulae of magnetite samples were Fe_3O_4, $Fe_{2.02}Ti_{0.98}O_4$, $Fe_{2.04}Cr_{0.96}O_4$, $Fe_{2.15}Mn_{0.85}O_4$, $Fe_{2.19}Co_{0.91}O_4$ and Fe_2NiO_4, labeled as M, Ti-M, Cr-M, Mn-M, Co-M and Ni-M, respectively. The iron content decreased after the incorporation of transition metals, indicating that these metals have replaced iron in the inverse spinel structure. The molar ratio between iron and substituting metal was close to 2:1, suggesting that these samples were on a similar substitution level.

The PXRD patterns (Fig. 1) of magnetite samples well corresponded to the standard card of magnetite (JCPDS: 19-0629). For substituted magnetite samples, both the broadening of diffraction lines at ca. 28–39° and the shift of peaks at ca. 35.5° toward lower diffraction angle indicate the incorporation of substituting metals into inverse spinel structure, which is resulted from the difference in ionic radii between iron and substituting metal cations (Table 1). For Ni-M, its PXRD pattern suggested the presence of magnetite with slightly poor crystallinity and another phase of iron chloride hydroxide (JCPDS: 49-0095, not shown) with the weak reflections at 11.4°, 23.0°, 33.4° and 37.5°, respectively. From the electron

Table 1
The valence and occupancy of substituting cations in magnetite.

Substituted cations	Valence	Ionic radius (Å)	Occupancy
Ti	+4	0.60	Octahedron
Cr	+3	0.63	Octahedron
Mn	+2	0.80 [23]	Tetrahedron
	+3	0.65 [24]	Octahedron
Co	+2	0.74 [23]	Octahedron
Ni	+2	0.70 [23]	Octahedron

probe analysis results (not shown), chlorine content in Ni-M was less than 0.1%, indicating that the presence of iron chloride hydroxide phase could be ignored.

XANES results (Table 1) showed that the substituting cations (Ti^{4+}, Cr^{3+}, Mn^{3+}, Co^{2+}, and Ni^{2+}) mainly occupied the octahedral sites of magnetite while Mn^{2+} occupied the tetrahedral ones. The detailed discussion of XANES results obtained in this study has been presented elsewhere [21]. According to the isomorphous replacement principle, Ti^{4+} replaced Fe^{3+} with the same amount of Fe^{3+} changed to Fe^{2+} for electrovalence equilibrium [25]. For Cr^{3+} and bivalent cations, e.g. Co^{2+} and Ni^{2+}, they mainly substituted Fe^{3+} and Fe^{2+}, respectively, without any iron oxidation or reduction. But for Mn, Mn cations coexisted as Mn^{2+} and Mn^{3+}, and occupied the tetrahedral and octahedral sites, which was consistent with the previous study by Denecke [26].

The specific surface areas of M, Ti-M, Cr-M, Mn-M, Co-M and Ni-M were 18.9, 57.1, 110.0, 21.4, 9.2 and 52.8 $m^2\ g^{-1}$, respectively. The isomorphous substitutions obviously changed the specific surface area of magnetite. The introduction of Ti, Cr, Mn and Ni increased the specific surface area whereas there was a dramatical decrease in the case of Co. Among these samples, Cr-M had the largest specific surface area, followed by Ti-M and Ni-M.

The amount of surface hydroxyl in magnetite samples was determined by TG-DSC analysis. As shown by the TG curves, two mass losses were observed from ca. 30 °C to 500 °C, corresponding to the dehydration and dehydroxylation processes (Fig. 2a). For sample M, its mass loss in dehydroxylation process was 0.48%, with peak centered at 271 °C on the derivative thermogravimetry (DTG) trace (Fig. 2b). For samples Ti-M, Cr-M, Mn-M, Co-M and Ni-M, their DTG peaks related to dehydroxylation were centered at ca. 156, 246, 231, 391 and 271 °C, with mass losses of 4.40%, 6.59%, 1.27%, 1.65% and 7.87%, respectively. Co substitution greatly increased the dehydroxylation temperature, while other metals showed a reverse effect. But all the substituting metals obviously increased the surface hydroxyl amount. Ni-M had the highest surface hydroxyl amount and was followed by Cr-M and Ti-M.

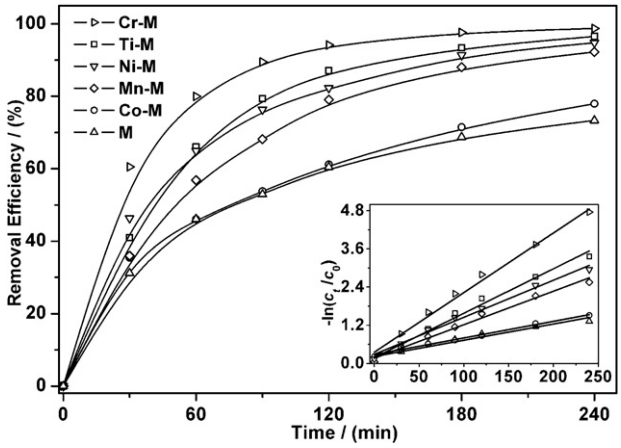

Fig. 3. Kinetic process of TBBPA degradation in UV/Fenton reaction catalyzed by $Fe_{3-x}M_xO_4$. Inset: Fitted by pseudo-first-order equation (TBBPA: 20 mg L^{-1}, H_2O_2: 10 mmol L^{-1}, catalyst: 0.50 g L^{-1}; 500 mL, pH: 6.5, 25 °C).

Table 2
The kinetic parameters of TBBPA UV/Fenton degradation.

Samples	k_{app} ($\times 10^{-3}$ min^{-1})	$t_{1/2}$ (min)
M	5.1	93.0
Ti-M	14.0	36.7
Cr-M	18.7	18.2
Mn-M	10.5	50.2
Co-M	5.2	79.6
Ni-M	11.7	35.1

3.2. TBBPA degradation

The UV/Fenton catalytic activity of magnetite samples was investigated in the degradation of TBBPA (Fig. 3). All the degradation processes were well fitted by the pseudo-first-order rate equation (Eq. (1)) with correlation coefficient higher than 0.96 (Fig. 3).

$$-ln\frac{C_t}{C_0} = k_{app}t \quad (1)$$

where C_0 and C_t were the TBBPA concentrations at the initial time and different reaction time t, mg L^{-1}. k_{app} was the apparent pseudo-first-order rate constant, min^{-1}.

Table 2 shows the rate constant k_{app} and half-life $t_{1/2}$ for TBBPA degradation in Fig. 3. Among these processes, TBBPA degradation catalyzed by Cr-M was the fastest. The k_{app} was 0.0187 min^{-1}, 3.7

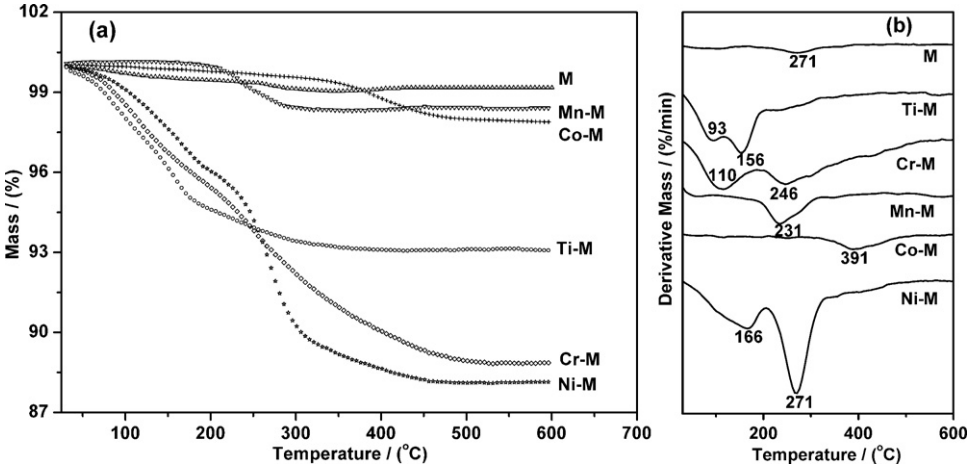

Fig. 2. TG (a) and DTG (b) curves of the synthetic $Fe_{3-x}M_xO_4$ under N_2 atmosphere.

times more than that by M. On the contrast, k_{app} for Co-M catalyzed process was much lower, 0.0052 min^{-1}, quite close to that for M contained system.

Compared to rate constant k_{app}, the $t_{1/2}$ value was more evident to show the difference in catalytic activity among substituted magnetites (Table 2). For magnetite M, about 93.0 min was needed to degrade 50% of TBBPA in reaction solution. For substituted samples, the $t_{1/2}$ for TBBPA degradation was fewer than that by sample M, indicating that the incorporation of these transition metals improved catalytic activity of magnetite in UV/Fenton reaction. Among these substituted samples, Cr-M had the strongest catalytic activity for TBBPA degradation, with the minimum value of $t_{1/2}$ (18.2 min). Although the k_{app} for Co-M catalyzed process was close to that by sample M, the $t_{1/2}$ for Co-M containing system was 79.6 min, obviously shorter than that for M containing system (93.0 min). According to the $t_{1/2}$ value, the improvement extent of these substituting metals on the UV/Fenton catalytic activity of magnetite increased in the following order: Co < Mn < Ti ≈ Ni < Cr. After 240 min degradation, the pH of degradation systems catalyzed by all magnetites were in the range of 6.7–7.8, suggesting that TBBPA degradation by these substituted magnetites was mainly dominated by the heterogeneous UV/Fenton process [27].

Iron leaching was quite important for the application of magnetite as reusable catalyst. According to previous study [15], though Ti-M had good stability and reusability, its dissolved iron concentration was proportional to the reaction time, which slightly decreased the catalytic activity of magnetite. In the present study, the concentration of leaching iron was also tracked. The final concentration of dissolved iron in Cr-M contained system was below the detection limit, also indicating that TBBPA degradation by Cr-M was mainly the heterogeneous process. Compared to Ti-M, Cr-M exhibited higher catalytic activity and overcome the drawback of leaching iron. From this point of view, Cr-M may be a more promising catalyst for the treatment of TBBPA wastewater through heterogeneous UV/Fenton reaction.

3.3. Transformation products of TBBPA

To further compare the catalytic activity of substituted magnetites in heterogeneous UV/Fenton reaction, the degradation products of TBBPA in three systems catalyzed by M, Ti-M and Cr-M were identified by GC–MS.

The concentrations of detected degradation products were semiquantitatively determined by comparing their relative peak area response to that of TBBPA. Our previous study has proposed the degradation pathways of TBBPA in heterogeneous UV/Fenton reaction catalyzed by titanomagnetite ($Fe_{3-x}Ti_xO_4$) [15]. TBBPA underwent the sequential debromination to form tribromobisphenol A (TriBBPA), dibromobisphenol A (DiBBPA), monobromobisphenol A (MonoBBPA) and bisphenol A (BPA), and β-scission to generate seven brominated compounds (Products **2–13** in Fig. 4 and Table 3). In the system containing M (Fig. 4), eight intermediate products were found after 240 min degradation. About 40% (relative percentage composition) of TBBPA were undegraded and about 45% of the products were TriBBPA, suggesting that the dominant degradation pathway of TBBPA in this system stayed in the stage of releasing the first bromine. Compared to M and Ti-M, only six products were found in the system containing Cr-M (Fig. 4). Obviously, TBBPA degradation in Cr-M contained system was more complete than other two systems, which also indicated the higher catalytic activity of Cr-M. The six residual products in Cr-M catalyzed system were identified as phenol (94, 62.98%) (molecular weight, relative peak area of the products), 4-(2-hydroxyisopropyl)-2,6-dibromophenol (310, 6.14%), 4-isopropyl-2,6-dibromophenol (294, 2.00%), MonoBBPA (308, 9.32%), DiBBPA (386, 8.34%) and TriBBPA (464, 11.22%). It is noteworthy that these products can be finally mineralized in the reaction system.

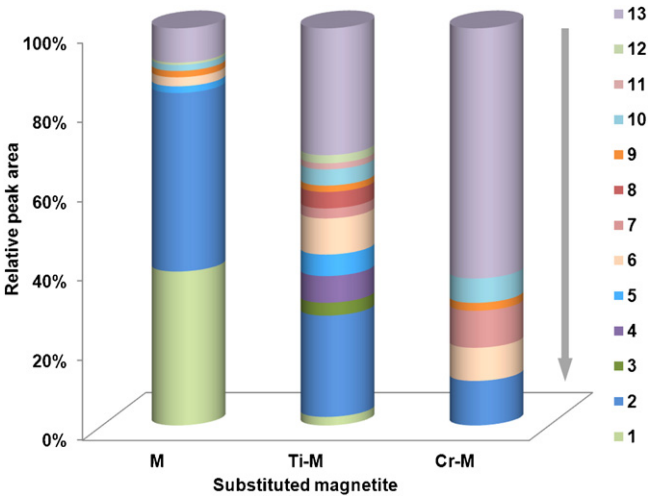

Fig. 4. The residual products composition of TBBPA degradation in heterogeneous UV/Fenton reaction catalyzed by substituted magnetites after 240 min (The direction of arrow shows the sequence of peaks in GC–MS, the number **1** represents TBBPA, **2–13** represents the products).

3.4. Effect of substitution on TBBPA degradation

In the present study, the presence of transition metal cations, i.e. Ti^{4+}, Cr^{3+}, Mn^{2+}/Mn^{3+}, Co^{2+} and Ni^{2+}, in the inverse spinel structure obviously enhanced the catalytic activity of magnetite in TBBPA degradation. From previous studies, the titanium substitution improved the electron transfer process in inverse spinel structure and the crystal properties of magnetite, e.g. formation of defects, dislocation and oxygen vacancies [28,29]. These varieties accelerated the generation of hydroxyl free radical (•OH), thereby increasing the TBBPA degradation efficiency. Moreover, some substitutions changed the surface properties of magnetite, e.g. specific surface area and surface hydroxyl amount [21]. This enhanced the adsorption of organic pollutants and H_2O_2, which also accelerated the degradation process. Therefore, in the present study, the distinct effects of studied substitutions on the catalytic activity of magnetite were interpreted in terms of both catalytic mechanism and surface properties.

3.4.1. Effect of substitution on UV/Fenton catalytic activity of magnetite

In the UV/Fenton reaction catalyzed by magnetite, organic pollutants were degraded mainly by •OH radicals, the most active oxidant with a quite high redox potential. •OH radical was generated by the reaction between $\equiv Fe^{II}$ on magnetite surface and H_2O_2 through the Haber Weiss mechanism (Eq. (2)) and the photolysis of H_2O_2 (Eq. (3)).

$$Fe^{2+} + H_2O_2 \rightarrow Fe^{3+} + {}^{\bullet}OH + OH^- \quad (2)$$

$$H_2O_2 + h\nu \rightarrow 2{}^{\bullet}OH \quad (3)$$

Previous studies indicated that some substituting cations on magnetite surface participated in the generation of •OH radicals (Eq. (4)) [30]:

$$\equiv M^{n+} + H_2O_2 \rightarrow \equiv M^{n+1} + 2{}^{\bullet}OH \quad (4)$$

where $\equiv M^{n+}$ donated the transition metal cations on magnetite surface. In a thermodynamic point of view, not all the cations in this study participated in Eq. (4), ascribed to their distinct oxidation potentials (Eqs. (5)–(9)). For Co^{2+} substitution, the oxidation

Table 3
The transformation products of TBBPA [15].

Products	RT (min)	WM	Proposed name
1	31.76	544	TBBPA
2	27.64	464	TriBBPA
3	26.48	430	Dibromo-4-[2-(4-hydroxy phenyl)] isopropoxy benzoic acid
4	26.17	430	Dibromo-4-[2-(4-hydroxy phenyl)] isopropoxy benzoic acid
5	26.05	386	DiBBPA
6	23.03	386	DiBBPA
7	21.24	308	MonoBBPA
8	17.90	358	2-(2,4-cyclopentadienyl)-2-(3,5-dibromo-4-hydroxyphenyl) propane
9	12.19	294	4-isopropyl-2,6-dibromophenol
10	11.61	310	4-(2-hydroxyisopropyl)-2,6-dibromophenol
11	10.59	228	BPA
12	9.67	292	4-isopropylene-2,6-dibromophenol
13	8.03	94	Phenol

potential value of redox pair Co^{2+}/Co^{3+} (1.81 V) was higher than that of H_2O_2 (1.776 V) [31], resulting in the Fenton-like process catalyzed by Co^{2+} thermodynamically unfavorable (Eq. (9)). In contrast, Ti^{4+}, Cr^{3+}, Mn^{2+} and Ni^{2+} with redox pairs Ti^{3+}/Ti^{4+} (−0.099 V), Cr^{2+}/Cr^{3+} (0.408 V), Mn^{2+}/Mn^{3+} (−1.51 V), and Ni^{2+}/Ni^{3+} (−1.74 V), respectively, displayed oxidation potentials lower than that of H_2O_2, illustrating that they could initiate the Fenton-like process and produce •OH radicals (Eqs. (5)–(8)). For example, the Cr substitution improved the electron transfer process between Cr_{surf}^{3+} and Fe_{surf}^{2+} to form Cr_{surf}^{2+} [9], which had the highest activity in •OH generation among the studied substitutions (Eq. (6)). Such an effect made Cr-M more efficient for •OH generation than other substituted magnetites. With lower potential difference value (Eqs. (5)–(8)), the catalytic activity of samples Ti-M, Ni-M and Mn-M in UV/Fenton degradation of TBBPA was weaker than that of Cr-M. However, the decrease trend of catalytic activity does not completely follow their potential difference. For example, although the •OH generation process was thermodynamically unfavorable for Co-M, Co substitution improved the catalytic activity of magnetite. This implies that another improvement mechanism may exist for these substitutions.

$$Ti_{surf}^{3+} + H_2O_2 \rightarrow Ti_{surf}^{4+} + {}^{\bullet}OH + OH^-,\ \Delta E = 1.677\,V \quad (5)$$

$$Cr_{surf}^{2+} + H_2O_2 \rightarrow Cr_{surf}^{3+} + {}^{\bullet}OH + OH^-,\ \Delta E = 2.184\,V \quad (6)$$

$$Mn_{surf}^{2+} + H_2O_2 \rightarrow Mn_{surf}^{3+} + {}^{\bullet}OH + OH^-,\ \Delta E = 0.266\,V \quad (7)$$

$$Ni_{surf}^{2+} + H_2O_2 \rightarrow Ni_{surf}^{3+} + {}^{\bullet}OH + OH^-,\ \Delta E = 0.036\,V \quad (8)$$

$$Co_{surf}^{2+} + H_2O_2 \rightarrow Co_{surf}^{3+} + {}^{\bullet}OH + OH^-,\ \Delta E = -0.0346\,V \quad (9)$$

The possible mechanism for the active substitution is their inhibitory effect for the combination of photo-induced electrons (e^-) and holes (h^+). Under UV irradiation, the electrons (e^-) and holes (h^+) quite easy to be generated on magnetite surface, but they were unstable and recombined quite quickly within a few nanoseconds [32]. From previous researches [30,33], some substituting cations created the oxygen vacancies [28,29], which were shallow traps to inhibit the recombination of photo-generated electrons and holes (Eq. (10)), and thus prolonged the lifetime of charge carriers [34,35].

$$M^{n+} + ze^- \rightarrow M^{(n-z)+} \quad (10)$$

where M represented transition metal cations.

3.4.2. *Effect of substitution on surface properties of magnetite*

Specific surface area greatly affected the catalytic activity of magnetite [36], as the contact frequency between magnetite and reactant molecules quickened with the increase of specific surface area of catalyst. In this study, the degradation efficiency of TBBPA by magnetites was well positively correlated to their specific surface area (Fig. 5). Among the substituted magnetite samples, Cr-M

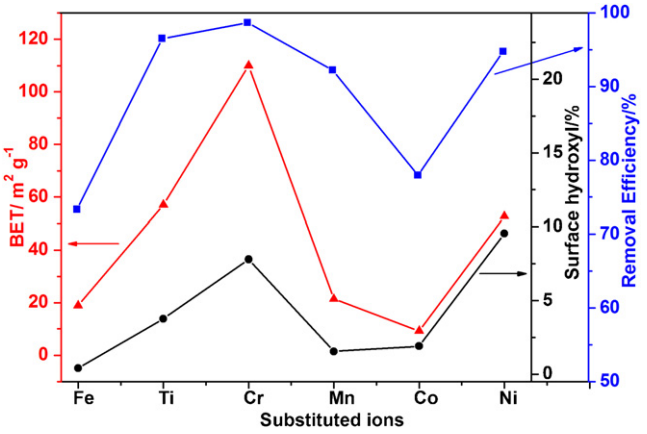

Fig. 5. Effect of specific surface area and surface hydroxyl amount of the substituted magnetites on the degradation efficiency of TBBPA.

with the strongest catalytic activity for TBBPA degradation showed the largest surface area of 110.0 $m^2\ g^{-1}$, while Co-M with the lowest catalytic activity had the smallest surface area of around 9.2 $m^2\ g^{-1}$. The variation tendency of catalytic efficiency was quite similar to that of specific surface area, suggesting that the difference of specific surface area was an important reason for the distinct effect of the studied substitutions on catalytic activity of magnetite.

The surface hydroxyl groups are functional groups of iron oxides, due to its vital role in surface adsorption [37], photocatalysis [38] and surface acidity (Brønsted acid) [39]. The incorporation of substituting metals resulted in a slight distortion of magnetite lattice and accordingly increased the surface hydroxyl amount [40]. The superficial hydroxyl groups can directly accept photo-generated holes [41,42] and adsorb H_2O_2 to produce •OH simultaneously [43,44]. As shown in Fig. 5, the variation tendency of TBBPA degradation efficiency by substituted magnetites corresponded roughly to that of surface hydroxyl amount. Sample Cr-M with the highest surface hydroxyl amount displayed strongest catalytic activity in TBBPA degradation. The surface hydroxyl amount of Co-M was about 2% in mass, a bit higher than that of M, below 0.5% in mass, which should be the possible reason for the higher catalytic activity of Co-M than that of M.

Based on the above discussion, the difference in surface property variety should be another reason for the distinct effects of the studied substitutions on the catalytic performance of magnetite in TBBPA degradation.

4. Conclusions

The heterogeneous UV/Fenton degradation of TBBPA catalyzed by transition metal substituted magnetites $Fe_{3-x}M_xO_4$ (M = Ti,

Cr, Mn, Co and Ni) was investigated. The incorporation of the investigated cations improved the UV/Fenton catalytic activity of magnetite, and the improvement extent increased in the following order: Co < Mn < Ti ≈ Ni < Cr. All the degradation processes were well fitted by the pseudo-first-order equation in kinetics. The substituting cations enhanced the UV/Fenton catalytic activity mainly by directly participating in the Fenton-like reaction to produce •OH radicals and increasing the specific surface area and surface hydroxyl amount. The above results are of high importance for well understanding the effect of isomorphous substitution on the UV/Fenton catalytic activity of magnetite, and prospecting the development of magnetite minerals for environmental purification application.

Acknowledgements

This is contribution No. IS-1611 from GIG CAS. We would like to thank Shanghai Synchrotron Radiation Facility (SSRF) for providing us the beam time for the XANES measurement. This work was financially supported by the National Natural Science Foundation of China (Grant Nos. 41172045 and 41103056) and Shanghai Tongji Gao Tingyao Environmental Science & Technology Development Foundation (STGEF).

References

[1] R.C.C. Costa, F.C.C. Moura, J.D. Ardisson, J.D. Fabris, R.M. Lago, Appl. Catal. B: Environ. 83 (2008) 131–139.
[2] M. Usman, P. Faure, C. Ruby, K. Hanna, Chemosphere 87 (2012) 234–240.
[3] S.P. Sun, A.T. Lemley, J. Mol. Catal. A: Chem. 349 (2011) 71–79.
[4] S. Anandan, G.J. Lee, S.H. Hsieh, M. Ashokkumar, J.J. Wu, Ind. Eng. Chem. Res. 50 (2011) 7874–7881.
[5] X.B. Luo, C.C. Wang, S.L. Luo, R.Z. Dong, X.M. Tu, G.S. Zeng, Chem. Eng. J. 187 (2012) 45–52.
[6] A.F. Ngomsik, A. Bee, M. Draye, G. Cote, V. Cabuil, C.R. Chim. 8 (2005) 963–970.
[7] S. Lee, J. Oh, Y. Park, Bull. Kor. Chem. Soc. 27 (2006) 489–494.
[8] S.J. Yang, H.P. He, D.Q. Wu, D. Chen, X.L. Liang, Z.H. Qin, M.D. Fan, J.X. Zhu, P. Yuan, Appl. Catal. B: Environ. 89 (2009) 527–535.
[9] F. Magalhaes, M.C. Pereira, S.E.C. Botrel, J.D. Fabris, W.A. Macedo, R. Mendonca, R.M. Lago, L.C.A. Oliveira, Appl. Catal. A: Gen. 332 (2007) 115–123.
[10] R.C.C. Costa, M.F.F. Lelis, L.C.A. Oliveira, J.D. Fabris, J.D. Ardisson, R.R.V.A. Rios, C.N. Silva, R.M. Lago, J. Hazard. Mater. 129 (2006) 171–178.
[11] M.A. Nejad, M. Jonsson, J. Nucl. Mater. 334 (2004) 28–34.
[12] M. Sorescu, A. Grabias, D. Tarabasanu-Mihaila, L. Diamandescu, J. Appl. Phys. 91 (2002) 8135–8137.
[13] L.C.A. Oliveira, J.D. Fabris, R.R.V.A. Rios, W.N. Mussel, R.M. Lago, Appl. Catal. A: Gen. 259 (2004) 253–259.
[14] C.G. Ramankutty, S. Sugunan, Appl. Catal. A: Gen. 218 (2001) 39–51.
[15] Y.H. Zhong, X.L. Liang, Y. Zhong, J.X. Zhu, S.Y. Zhu, P. Yuan, H.P. He, J. Zhang, Water Res. 46 (2012) 4633–4644.
[16] S. Kitamura, N. Jinno, S. Ohta, H. Kuroki, N. Fujimoto, Biochem. Biophys. Res. Commun. 293 (2002) 554–559.
[17] L.S. Birnbaum, D.F. Staskal, Environ. Health Persp. 112 (2004) 9–17.
[18] K.D. Lin, W.P. Liu, J. Gan, Environ. Sci. Technol. 43 (2009) 4480–4486.
[19] S. Luo, S.G. Yang, C. Sun, X.D. Wang, Water Res. 45 (2011) 1519–1528.
[20] W. Yu, T.L. Zhang, J.G. Zhang, X.J. Qiao, L. Yang, Y.H. Liu, Mater. Lett. 60 (2006) 2998–3001.
[21] X.L. Liang, Y.H. Zhong, W. Tan, J.X. Zhu, P. Yuan, H.P. He, Z. Jiang, J. Therm. Anal. Calorim. (2012) 1–8.
[22] J.X. Chen, L.Z. Zhu, J. Photochem. Photobiol. A 188 (2007) 56–64.
[23] P.S. Sidhu, R.J. Gilkes, A.M. Posner, J. Inorg. Nucl. Chem. 40 (1978) 429–435.
[24] G. Pistoia, A. Antonini, R. Rosati, C. Bellitto, G.M. Ingo, Chem. Mater. 9 (1997) 1443–1450.
[25] C.I. Pearce, C.M.B. Henderson, N.D. Telling, R.A.D. Pattrick, J.M. Charnock, V.S. Coker, E. Arenholz, F. Tuna, G. van der Laan, Am. Mineral. 95 (2010) 425–439.
[26] M.A. Denecke, W. Gunsser, G. Buxbaum, P. Kuske, Mater. Res. Bull. 27 (1992) 507–514.
[27] S.S. Chou, C.P. Huang, Y.H. Huang, Environ. Sci. Technol. 35 (2001) 1247–1251.
[28] H.M. Liu, W.S. Yang, Y. Ma, Y. Cao, J.N. Yao, J. Zhang, T.D. Hu, Langmuir 19 (2003) 3001–3005.
[29] M. Anpo, M. Che, B. Fubini, E. Garrone, E. Giamello, M.C. Paganini, Top. Catal. 8 (1999) 189–198.
[30] M.I. Litter, Appl. Catal. B: Environ. 23 (1999) 89–114.
[31] K. Hernadi, A. Siska, L. Thien-Nga, L. Forro, I. Kiricsi, Solid State Ionics 141 (2001) 203–209.
[32] M. Buchler, P. Schmuki, H. Bohni, T. Stenberg, T. Mantyla, J. Electrochem. Soc. 145 (1998) 378–385.
[33] K. Nagaveni, M.S. Hegde, G. Madras, J. Phys. Chem. B 108 (2004) 20204–20212.
[34] Y. Yang, X.J. Li, J.T. Chen, L.Y. Wang, J. Photochem. Photobiol. A 163 (2004) 517–522.
[35] S.D. Sharma, D. Singh, K.K. Saini, C. Kant, V. Sharma, S.C. Jain, C.P. Sharma, Appl. Catal. A: Gen. 314 (2006) 40–46.
[36] J. Bandara, J.A. Mielczarski, J. Kiwi, Langmuir 15 (1999) 7670–7679.
[37] Y. Zhang, M. Yang, X.M. Dou, H. He, D.S. Wang, Environ. Sci. Technol. 39 (2005) 7246–7253.
[38] K. Nagaveni, G. Sivalingam, M.S. Hedge, G. Madras, Appl. Catal. B: Environ. 48 (2004) 83–93.
[39] Y.H. Zhang, G.X. Xiong, N. Yao, W.S. Yang, X.Z. Fu, Catal. Today 68 (2001) 89–95.
[40] U. Schwertmann, E. Wolska, Clay Clay Miner. 38 (1990) 209–212.
[41] V. Augugliaro, M. Pagliaro, V. Loddo, G. Palmisano, L. Palmisano, Clean by Light Irradiation: Practical Applications of Supported TiO_2, Royal Society of Chemistry, Cambridge, 2010, 19 pp.
[42] D. Nassoko, Y.F. Li, J.L. Li, X. Li, Y. Yu, Int. J. Photoenergy 2012 (2012) 1–10.
[43] S.S. Lin, M.D. Gurol, Environ. Sci. Technol. 32 (1998) 1417–1423.
[44] E.G. Garrido-Ramirez, B.K.G. Theng, M.L. Mora, Appl. Clay Sci. 47 (2010) 182–192.